

## Conservative Semi-Lagrangian Finite Difference WENO Formulations with Applications to the Vlasov Equation

Jing-Mei Qiu<sup>1,\*</sup> and Chi-Wang Shu<sup>2</sup>

<sup>1</sup> *Department of Mathematical and Computer Science, Colorado School of Mines,  
Golden, CO 80401, USA.*

<sup>2</sup> *Division of Applied Mathematics, Brown University, Providence, RI 02912, USA.*

Received 18 February 2010; Accepted (in revised version) 25 November 2010

Available online 22 June 2011

---

**Abstract.** In this paper, we propose a new conservative semi-Lagrangian (SL) finite difference (FD) WENO scheme for linear advection equations, which can serve as a base scheme for the Vlasov equation by Strang splitting [4]. The reconstruction procedure in the proposed SL FD scheme is the same as the one used in the SL finite volume (FV) WENO scheme [3]. However, instead of inputting cell averages and approximate the integral form of the equation in a FV scheme, we input point values and approximate the differential form of equation in a FD spirit, yet retaining very high order (fifth order in our experiment) spatial accuracy. The advantage of using point values, rather than cell averages, is to avoid the second order spatial error, due to the shearing in velocity ( $v$ ) and electrical field ( $E$ ) over a cell when performing the Strang splitting to the Vlasov equation. As a result, the proposed scheme has very high spatial accuracy, compared with second order spatial accuracy for Strang split SL FV scheme for solving the Vlasov-Poisson (VP) system. We perform numerical experiments on linear advection, rigid body rotation problem; and on the Landau damping and two-stream instabilities by solving the VP system. For comparison, we also apply (1) the conservative SL FD WENO scheme, proposed in [22] for incompressible advection problem, (2) the conservative SL FD WENO scheme proposed in [21] and (3) the non-conservative version of the SL FD WENO scheme in [3] to the same test problems. The performances of different schemes are compared by the error table, solution resolution of sharp interface, and by tracking the conservation of physical norms, energies and entropies, which should be physically preserved.

**AMS subject classifications:** 65

**Key words:** Semi-Lagrangian methods, finite difference/finite volume scheme, conservative scheme, WENO reconstruction, Vlasov equation, Landau damping, two-stream instability.

---

\*Corresponding author. *Email addresses:* jingqiu@mines.edu (J.-M. Qiu), shu@dam.brown.edu (C.-W. Shu)

## 1 Introduction

In this paper, we propose a conservative semi-Lagrangian (SL) finite difference (FD) WENO scheme, by utilizing the same reconstruction procedure as in the SL finite volume (FV) WENO scheme in [3] for solving the 1-D advection equation

$$u_t + cu_x = 0, \quad \text{where } c \text{ is a constant.} \quad (1.1)$$

This work is motivated by the kinetic plasma applications, where the Vlasov equation is often numerically solved by the following procedure. First, the Strang splitting is applied to decouple the high-dimensional nonlinear Vlasov equation into a sequence of linear advection equations, such as (1.1); then a SL scheme is applied to solve those decoupled 1-D equations. The SL approach for solving the Strang splitted Vlasov equation has been very popular in the plasma simulation community, see for example [3, 9, 12, 21, 27, 31], as the scheme for the splitted 1-D equation is usually simple, effective and free of CFL condition, which is a restriction in Eulerian approach. There are many variance in designing a SL scheme. Specifically, we characterize a SL scheme by the following three key components:

1. *A solution space.* The solution space can be point values, integrated mass (cell averages), or a piecewise polynomial function living on a fixed numerical grid, corresponding to the SL FD scheme [3, 15, 21], SL FV scheme [9, 12] and the characteristic Galerkin method [5, 17] respectively.
2. *Propagation.* In each of the time step evolution, information is propagated along characteristics. Usually, a high order interpolation or reconstruction procedure, which determines the spatial accuracy of the scheme, is applied to recover the information among discrete information on the solution space. In the literature, there are a variety of interpolation/reconstruction choices, such as the piecewise parabolic method (PPM) [7], positive and flux conservative method (PFC) [13], spline interpolation [8], cubic interpolation propagation (CIP) [28], ENO/WENO interpolation or reconstruction [3, 16, 21, 22, 26]. We refer to [9, 10, 29] for comparison of different reconstruction procedures.
3. *Projection.* Lastly, the evolved solution is projected back onto the solution space, updating the numerical solution at  $t^{n+1}$ .

It is known that the mass conservation is a very important property of a SL scheme. Failure to conserve the mass might lead to some instability of the scheme [15]. To conserve the mass, a scheme working with integrated mass in a FV spirit, seems more natural and straightforward [9]. On the other hand, we argue that it is advantageous to work with point values (FD scheme), rather than cell averages (FV scheme), due to the shearing of advection coefficients ( $v$  and  $E$ ) over a cell, in the context of Strang splitting for Vlasov equation or other kinetic equations of similar kind. Due to above considerations, a conservative scheme that works with point values seems ideal [21, 22]. In this paper, we propose another approach of designing a conservative SL FD scheme by utilizing the

same WENO reconstruction procedure as in a SL FV scheme [3]. The idea is motivated by the very close relation between the FV and FD WENO scheme [16,26] for a semi-discrete equation. We compare the performance of proposed scheme with the conservative or non-conservative SL FD WENO schemes designed earlier in [3,21,22]. We note that the scheme in [22] is applied to advection in incompressible flow; while in this paper, the scheme in [22] is applied to Vlasov-Poisson (VP) system for the first time. Finally, we remark that the SL method that we proposed is for linear equations. The SL schemes for nonlinear equations are much more complicated and are out of the scope of the current paper. Especially, due to the formation of shocks, the forward characteristics might intersect with each other; or there might be multiple candidates for the root of characteristic from backward characteristics tracing. This impose difficulty in designing a robust and effective numerical scheme. We refer readers to [19,23,30] for research work in this direction.

The paper is organized as follows. Section 2 is a review of FV and FD WENO scheme for semi-discrete advection equation. Section 3 presents the SL FV WENO scheme [3], and the proposed conservative SL FD WENO scheme, based on the same WENO reconstruction procedure as in the SL FV WENO scheme. Section 4 compares the proposed scheme together with the conservative SL FD WENO scheme in [21,22] and non-conservative SL FD WENO scheme in [3] by linear advection and rigid body rotation. Section 5 demonstrates the performance of the proposed schemes, in comparison with other SL FD WENO schemes [3,21,22], through the classical Landau damping and two stream instabilities by solving the VP system. Section 6 gives the conclusions.

## 2 FV and FD WENO methods

In this section, we will briefly review the FV and FD WENO spatial discretization for a semi-discrete 1-D linear advection equation

$$u_t + (cu)_x = 0, \quad \text{on } [a,b], \quad (2.1)$$

with the initial condition  $u(x,t=0) = u_0(x)$ . For simplicity, we assume a periodic boundary condition. The purpose of this review section is to recall the WENO reconstruction procedures in the FV and FD schemes, serving as a preparation for establishing the very close relationship of the reconstruction procedures in SL FV and FD schemes in Section 3. The readers are referred to [6,26] for more details. In this paper, we adopt the following spatial discretization of the domain  $[a,b]$

$$a = x_{\frac{1}{2}} < x_{\frac{3}{2}} < \cdots < x_{N+\frac{1}{2}} = b, \quad (2.2)$$

where  $I_i = [x_{i-1/2}, x_{i+1/2}]$ ,  $i=1, \dots, N$ , are uniform numerical cells with centers  $x_i = (x_{i+1/2} + x_{i-1/2})/2$ , and cell sizes  $\Delta x = x_{i+1/2} - x_{i-1/2} = (b-a)/N$ . We use

$$\bar{u}_i = \frac{1}{\Delta x} \int_{I_i} u(\xi, t) d\xi$$

to denote the cell averages of the solution over  $I_i$  and use  $u_i = u(x_i, t)$  to denote the point value of the solution at  $x = x_i$ . We use  $\bar{u}_i^n$  and  $u_i^n$  to denote the cell average/point value of the solution over  $I_i$ /at  $x_i$  at time  $t = t^n$  respectively.

### 2.1 FV formulation

The FV scheme evolves the cell averages of the solution  $\bar{u}_i, i = 1, \dots, N$ , by approximating the integral form of the Eq. (2.1)

$$\frac{d}{dt} \bar{u}_i = -\frac{1}{\Delta x} (\hat{f}_{i+\frac{1}{2}} - \hat{f}_{i-\frac{1}{2}}), \quad \forall i = 1, \dots, N, \tag{2.3}$$

where the numerical flux

$$\hat{f}_{i+\frac{1}{2}} = \hat{f}(u_{i+\frac{1}{2}}^-, u_{i+\frac{1}{2}}^+)$$

is consistent with the physical flux  $f(u) = cu$ . It is Lipschitz continuous and monotonically increasing/decreasing with respect to the first/second argument. For example, an upwind flux would be  $\hat{f}_{i+1/2} = cu_{i+1/2}^-$ , if  $c > 0$ ; and  $\hat{f}_{i+1/2} = cu_{i+1/2}^+$  otherwise. The values of  $u_{i+1/2}^\pm$  can be reconstructed in a WENO fashion from the cell averages in a neighborhood stencil  $\{u_{i-p}, \dots, u_{i+q}\}$ . Specifically, one more point from the left ( $p=q$ ) will be taken to reconstruct  $u_{i+1/2}^-$ , and one more point from the right ( $p=q-2$ ) will be taken to reconstruct  $u_{i+1/2}^+$ . We refer to [6,26] for the details of WENO reconstructions. In the method of line (MOL) procedure, the time derivative on the L.H.S of Eq. (2.3) is discretized by a stable time integrator, such as the third order strong stability preserving (SSP) Runge-Kutta (RK) method [14]. There are other types of time discretization available in the literature, e.g., the Lax-Wendroff type in [24].

### 2.2 FD formulation

The FD scheme evolves the point values of the solution  $u_i, i = 1, \dots, N$ , by approximating the Eq. (2.1) directly. The scheme is of conservative form

$$\frac{d}{dt} u_i = -\frac{1}{\Delta x} (\hat{f}_{i+\frac{1}{2}} - \hat{f}_{i-\frac{1}{2}}). \tag{2.4}$$

To obtain a high order approximation, a sliding average function  $h(x)$  is introduced, such that

$$\frac{1}{\Delta x} \int_{x-\frac{\Delta x}{2}}^{x+\frac{\Delta x}{2}} h(\xi) d\xi = cu(x, t). \tag{2.5}$$

Taking the  $x$  derivative of the above equation gives

$$\frac{1}{\Delta x} \left( h\left(x + \frac{\Delta x}{2}\right) - h\left(x - \frac{\Delta x}{2}\right) \right) = (cu)_x. \tag{2.6}$$

Therefore the numerical flux  $\hat{f}_{i+1/2}$  in Eq. (2.4) can be taken as  $h(x_{i+1/2})$ , which can be reconstructed from neighboring cell averages of  $h(x)$ ,

$$\bar{h}_j = \frac{1}{\Delta x} \int_{I_j} h(\xi) d\xi \stackrel{(2.5)}{=} cu(x_j, t), \quad j = i-p, \dots, i+q,$$

by the WENO reconstruction [26]. The stencil  $\{u_{i-p}, \dots, u_{i+q}\}$  is chosen to be upwind biased. Specifically, when  $c \geq 0$ , one more point from the left ( $p = q$ ) will be taken to reconstruct  $\hat{f}_{i+1/2}$ ; when  $c < 0$ , one more point from the right ( $p = q - 2$ ) will be taken. Similar to Eq. (2.3), Eq. (2.4) is further discretized in time by a stable time integrator, such as the third order SSP RK method [14].

**Remark 2.1.** (About WENO reconstructions) Although FV and FD schemes are working with different quantities of the solution (cell averages and point values respectively), the WENO reconstruction procedure in the FV and FD schemes is the same. Specifically, the WENO reconstruction in both FV and FD schemes can be thought of as a blackbox, whose input consists of cell averages of a given function, and whose output consists of highly accurate point values of the same function at cell boundaries. The only difference is that in the FV scheme, the reconstruction procedure works with the unknown function  $u$  itself; but in the FD scheme, the reconstruction procedure works with a sliding average function  $h$  defined in Eq. (2.5). In fact, for the linear advection equation with constant coefficients, the numerical procedure of the FV and FD WENO schemes is exactly the same. The only difference between these two schemes in this case is in the initial condition (the FV scheme uses the cell averages of the initial condition while the FD scheme uses its point values).

### 3 The SL FV and FD WENO schemes

In this section, we will start with a description of the SL FV WENO scheme, originally introduced in [3]. We will briefly outline the scheme in Section 3.1, which will be closely related to the SL FD WENO scheme introduced in Section 3.2.

#### 3.1 SL FV WENO scheme

In a FV scheme, it is the cell averages of the solution  $\bar{u}_i$  that are being updated. A SL FV scheme is formulated based on the following observation: at each of the cell boundaries at time level  $t^{n+1}$ , say  $(x_{i+1/2}, t^{n+1})$ , there exists a backward characteristic line, denoted as  $\Gamma_{i+1/2}$ , with its foot located on time level  $t^n$  at  $y_{i+1/2}$ . Since there is no flux passing through the characteristics lines, due to the mass conservation, the cell averages of the solution can be updated by

$$\bar{u}_i^{n+1} \doteq \frac{1}{\Delta x} \int_{x_{i-\frac{1}{2}}}^{x_{i+\frac{1}{2}}} u(x, t^{n+1}) dx = \frac{1}{\Delta x} \int_{y_{i-\frac{1}{2}}}^{y_{i+\frac{1}{2}}} u(x, t^n) dx. \tag{3.1}$$

To evaluate the R.H.S of Eq. (3.1), we would like to locate  $y_{i\pm 1/2}$  and to reconstruct the integral by the given cell averages  $\{\bar{u}_i^n\}_{i=1}^N$ . For a linear advection equation, the characteristics are straight lines with slope  $1/c$ , therefore  $y_{i\pm 1/2} = x_{i\pm 1/2} - c\Delta t$ ; and the integral can be reconstructed by a WENO interpolation of the primitive function of  $u$ . More specifically, we let

$$U^n(x) = \int^x u(\xi, t^n) d\xi$$

to be the primitive function of  $u(x, t^n)$  with  $U(a) = 0$ , then

$$U_i^n \doteq U^n(x_i) = \Delta x \sum_{j=1}^i \bar{u}_j^n, \quad \text{and} \quad \frac{1}{\Delta x} \int_{y_{i-\frac{1}{2}}}^{y_{i+\frac{1}{2}}} u(x, t^n) dx = \frac{1}{\Delta x} (U^n(y_{i+\frac{1}{2}}) - U^n(y_{i-\frac{1}{2}})).$$

We reconstruct the point values of  $U$ , e.g.,  $U(y_{i+1/2})$ , from the grid point values of  $\{U_i^n\}_{i=1}^N$  by a WENO interpolation. The WENO interpolation algorithm has been discussed in [2, 20, 25]. The difference between the WENO interpolation in this SL FV framework and that in the literature, e.g., in [25], is that (i) to obtain a  $(2k+1)$ <sup>th</sup> order local truncation error, we need a  $(2k+2)$ -point stencil due to the  $1/\Delta x$  factor in Eq. (3.1), and (ii) the smoothness indicators in the WENO algorithm should be derived, taking into account of second and higher order derivatives of  $U(x)$ , rather than first and higher derivative of  $u(x)$  as in the WENO interpolation in [25].

In the following, we provide a sixth order WENO interpolation, giving a fifth order SL FV WENO scheme, as used in our simulations in Section 4 and 5. The goal is to construct  $U(x)$  for any  $x \in [x_{i-1}, x_i]$  (or  $\xi \doteq (x - x_i)/\Delta x \in [-1, 0]$ ) in the WENO fashion from a 6-point stencil  $S = \{U_{i-3}, U_{i-2}, U_{i-1}, U_i, U_{i+1}, U_{i+2}\}$ , which can be decomposed into three 4-point stencils

$$S_1 = \{U_{i-3}, U_{i-2}, U_{i-1}, U_i\}, \quad S_2 = \{U_{i-2}, U_{i-1}, U_i, U_{i+1}\}, \quad S_3 = \{U_{i-1}, U_i, U_{i+1}, U_{i+2}\}.$$

*Linear weight function*  $C_k(\xi)$ ,  $k=1, 2, 3$ . We denote  $Q(\xi)$  as the polynomial of degree 5 interpolating the point values in the 6-point stencil  $S$  and denote  $P_k(\xi)$  as the polynomial of degree 3 interpolating the point values in the stencil  $S_k$ . It is proved in [2] that there exist linear weights  $C_k(x)$ , which are actually polynomials of degree 2, such that

$$Q(x) = \sum_{k=1}^3 C_k(x) P_k(x).$$

In the sixth order case of our implementation, we have

$$Q(\xi) = (U_{i-3}, U_{i-2}, U_{i-1}, U_i, U_{i+1}, U_{i+2}) \begin{pmatrix} 0 & -\frac{1}{30} & 0 & \frac{1}{24} & 0 & -\frac{1}{120} \\ 0 & \frac{1}{4} & -\frac{1}{24} & -\frac{7}{24} & \frac{1}{24} & \frac{1}{24} \\ 0 & -1 & \frac{2}{3} & \frac{7}{12} & -\frac{1}{6} & -\frac{1}{12} \\ 1 & \frac{1}{3} & -\frac{5}{4} & -\frac{5}{12} & \frac{1}{4} & \frac{1}{12} \\ 0 & \frac{1}{2} & \frac{2}{3} & \frac{1}{24} & -\frac{1}{6} & -\frac{1}{24} \\ 0 & -\frac{1}{20} & -\frac{1}{24} & \frac{1}{24} & \frac{1}{24} & \frac{1}{120} \end{pmatrix} \begin{pmatrix} 1 \\ \xi \\ \xi^2 \\ \xi^3 \\ \xi^4 \\ \xi^5 \end{pmatrix},$$

$$\begin{aligned}
 P_1(\xi) &= (U_{i-3}, U_{i-2}, U_{i-1}, U_i) \begin{pmatrix} 0 & -\frac{1}{3} & -\frac{1}{2} & -\frac{1}{6} \\ 0 & \frac{3}{2} & 2 & \frac{1}{2} \\ 0 & -3 & -\frac{5}{2} & -\frac{1}{2} \\ 1 & \frac{11}{6} & 1 & \frac{1}{6} \end{pmatrix} \begin{pmatrix} 1 \\ \xi \\ \xi^2 \\ \xi^3 \end{pmatrix}, \\
 P_2(\xi) &= (U_{i-2}, U_{i-1}, U_i, U_{i+1}) \begin{pmatrix} 0 & \frac{1}{6} & 0 & -\frac{1}{6} \\ 0 & -1 & \frac{1}{2} & \frac{1}{2} \\ 1 & \frac{1}{2} & -1 & -\frac{1}{2} \\ 0 & \frac{1}{3} & \frac{1}{2} & \frac{1}{6} \end{pmatrix} \begin{pmatrix} 1 \\ \xi \\ \xi^2 \\ \xi^3 \end{pmatrix}, \\
 P_3(\xi) &= (U_{i-1}, U_i, U_{i+1}, U_{i+2}) \begin{pmatrix} 0 & -\frac{1}{3} & \frac{1}{2} & -\frac{1}{6} \\ 1 & -\frac{1}{2} & -1 & \frac{1}{2} \\ 0 & 1 & \frac{1}{2} & -\frac{1}{2} \\ 0 & -\frac{1}{6} & 0 & \frac{1}{6} \end{pmatrix} \begin{pmatrix} 1 \\ \xi \\ \xi^2 \\ \xi^3 \end{pmatrix}, \\
 C_1(\xi) &= \frac{1}{20}(\xi-1)(\xi-2), \quad C_2(\xi) = -\frac{1}{10}(\xi+3)(\xi-2), \quad C_3(\xi) = \frac{1}{20}(\xi+3)(\xi+2).
 \end{aligned}$$

Nonlinear weights by the smoothness indicator. The smoothness indicators  $\beta_k$  are determined by

$$\beta_k = \sum_{l=2}^3 \int_{-1}^0 \left( \frac{d^l}{d\xi^l} P_k(\xi) \right)^2 d\xi. \tag{3.2}$$

Therefore we have

$$\begin{aligned}
 \beta_1 &= -9U_{i-3}U_{i-2} + \frac{4}{3}U_{i-3}^2 - \frac{11}{3}U_{i-3}U_i + 10U_{i-3}U_{i-1} + 14U_{i-2}U_i \\
 &\quad + 22U_{i-1}^2 - 17U_{i-1}U_i + \frac{10}{3}U_i^2 + 16U_{i-2}^2 - 37U_{i-2}U_{i-1}, \\
 \beta_2 &= -7U_{i-2}U_{i-1} + \frac{4}{3}U_{i-2}^2 - \frac{5}{3}U_{i-2}U_{i+1} + 6U_{i-2}U_i + 6U_{i-1}U_{i+1} \\
 &\quad + 10U_i^2 - 7U_iU_{i+1} + \frac{4}{3}U_{i+1}^2 + 10U_{i-1}^2 - 19U_{i-1}U_i, \\
 \beta_3 &= -17U_{i-1}U_i + \frac{10}{3}U_{i-1}^2 - \frac{11}{3}U_{i-1}U_{i+2} + 14U_{i-1}U_{i+1} + 10U_iU_{i+2} \\
 &\quad + 16U_{i+1}^2 - 9U_{i+1}U_{i+2} + \frac{4}{3}U_{i+2}^2 + 22U_i^2 - 37U_iU_{i+1}.
 \end{aligned}$$

The nonlinear weights are chosen to be

$$w_k(\xi) = \frac{\tilde{w}_k(\xi)}{\sum_{k=1}^3 \tilde{w}_k(\xi)}, \quad \tilde{w}_k(\xi) = \frac{C_k(\xi)}{(\epsilon + \beta_k)^2},$$

where  $\epsilon$  is chosen to be  $10^{-6}$  in our simulations.

### 3.2 SL FD WENO scheme

In a FD scheme, it is the point values of the solution  $u_i$  that is being updated. There have been two different formulations of conservative SL FD WENO schemes in the literature [21, 22]. The one in [22] is advantageous over that in [21] in that the formulation in [22] can be applied to equations with variable coefficients; while the one in [21], based on the splitting of interpolation matrices, only applies to advection with constant coefficients. In this paper, we introduce another formulation of the SL FD WENO scheme, based on the SL FV WENO scheme formulated in Section 3.1. Specifically, we show that instead of working with cell averages of the solution in a SL FV WENO scheme, if we work with point values in a FD formulation using the same WENO reconstruction procedure, we retain high order accuracy (fifth order in our simulations). This new SL FD WENO scheme is simpler to implement than that in [22]. Unfortunately, as the SL FD WENO scheme in [21], our current formulation only applies to equations with constant coefficients.

It is known that at each of the grid points  $x_i$ , there exists a backward characteristic line with the foot located on the time level  $t^n$  at  $y_i = x_i - c\Delta t$  for linear advection equation with advection speed  $c$ . Along the characteristics, the solution is constant  $u(x_i, t^{n+1}) = u(x_i - c\Delta t, t^n)$ . If we directly apply some point value reconstruction, e.g., the WENO interpolation to update  $u(x_i, t^{n+1})$ , the numerical scheme is not necessarily conservative. To design a conservative SL FD scheme, we define an  $h(x, t)$  function as following,

$$\frac{1}{\Delta x} \int_{X(t; x - \frac{\Delta x}{2}, t^{n+1})}^{X(t; x + \frac{\Delta x}{2}, t^{n+1})} h(\xi, t) d\xi = u(x, t), \quad t \in [t^n, t^{n+1}], \quad (3.3)$$

where  $X(t; \xi, t^{n+1})$  are the characteristics curves over  $[t^n, t^{n+1}]$  ending at  $(\xi, t^{n+1})$ , i.e.,

$$\frac{dX(t)}{dt} = c, \quad X(t^{n+1}) = \xi.$$

From the Eq. (3.3), we know that

$$u_i^{n+1} = \frac{1}{\Delta x} \int_{x_{i-\frac{1}{2}}}^{x_{i+\frac{1}{2}}} h(\xi, t^{n+1}) d\xi, \quad \frac{1}{\Delta x} \int_{x_{i-\frac{1}{2}} - c\Delta t}^{x_{i+\frac{1}{2}} - c\Delta t} h(\xi, t^n) d\xi = u(x_i - c\Delta t, t^n).$$

Since  $u(x_i, t^{n+1}) = u(x_i - c\Delta t, t^n)$ , we have

$$\frac{1}{\Delta x} \int_{x_{i-\frac{1}{2}}}^{x_{i+\frac{1}{2}}} h(\xi, t^{n+1}) d\xi = \frac{1}{\Delta x} \int_{x_{i-\frac{1}{2}} - c\Delta t}^{x_{i+\frac{1}{2}} - c\Delta t} h(\xi, t^n) d\xi. \quad (3.4)$$

In other words, in order to update the point values of  $u$ , e.g.,  $u_j^{n+1}$  from  $u(x_i - c\Delta t, t^n)$ , it is equivalent to update the cell averages of  $h$ , e.g.,  $\int_{x_{i-1/2}}^{x_{i+1/2}} h(\xi, t^{n+1}) d\xi / \Delta x$  from some

integrated mass of  $h$  at  $t^n$  on the R.H.S. of Eq. (3.4). On the other hand, this integral can be reconstructed from the cell averages of  $h$ , since

$$\bar{h}_i = \frac{1}{\Delta x} \int_{x_{i-\frac{1}{2}}}^{x_{i+\frac{1}{2}}} h(\xi, t^n) d\xi \stackrel{(3.3)}{=} u_i^n,$$

in the same way as the WENO reconstruction in the SL FV WENO scheme described in the previous subsection.

**Remark 3.1.** (conservation) The conservation property of the scheme can be seen by

$$\Delta x \sum_{i=1}^N u_i^{n+1} = \Delta x \sum_{i=1}^N \bar{h}_i^{n+1} = \sum_{i=1}^N \int_{x_{i-\frac{1}{2}}^{-c\Delta t}}^{x_{i+\frac{1}{2}}^{-c\Delta t}} h(\xi, t^n) d\xi = \Delta x \sum_{i=1}^N \bar{h}_i^n = \Delta x \sum_{i=1}^n u_i^n,$$

if periodic boundary condition is assumed.

**Remark 3.2.** Unfortunately, the above formulation can not be applied to the equations with variable coefficients. The problem is that

$$u_i^n = \frac{1}{\Delta x} \int_{X(t^n; x_{i-\frac{1}{2}}, t^{n+1})}^{X(t^n; x_{i+\frac{1}{2}}, t^{n+1})} h(\xi, t) d\xi \neq \frac{1}{\Delta x} \int_{x_{i-\frac{1}{2}}}^{x_{i+\frac{1}{2}}} h(\xi, t^n) d\xi = \bar{h}_i^n.$$

In other words,  $u_i^n$  is not necessarily the cell averages of  $h$ ,  $\bar{h}_i^n$ . A conservative update via this route is therefore, if not impossible, highly non-trivial.

**Remark 3.3.** The SL FV/FD formulations for the linear advection equations with constant coefficients are equivalent to the Lax-Wendroff formulation with enough terms in the Taylor expansions. This is a different time discretization strategy from the SSP RK schemes.

## 4 Numerical tests

In this section, the SL FD schemes proposed in Section 3 (referred to as Method I) is tested for the simple cases of linear advection and rigid body rotation, together with the conservative SL FD schemes proposed in [21, 22] (referred as Method II and Method III respectively), and the non-conservative SL FD scheme proposed in [3] (referred as Method IV). All of the SL FD schemes are coupled with a fifth order WENO reconstruction/interpolation.

### 4.1 Test examples

**Example 4.1.** (One dimensional linear translation)

$$u_t + u_x = 0, \quad x \in [0, 2\pi]. \tag{4.1}$$

Table 1: Order of accuracy for (4.1) with  $u(x,t=0) = \sin(x)$  at  $T=20$ .  $CFL=2.2$ .

-	Method I		Method II		Method III		Method IV	
	error	order	error	order	error	order	error	order
40	1.18E-5	-	1.18E-5	-	1.31E-5	-	1.02E-5	-
80	3.63E-7	5.03	3.63E-7	5.03	4.04E-7	5.03	3.47E-7	4.88
120	4.74E-8	5.02	4.74E-8	5.02	5.27E-8	5.03	4.63E-8	4.96
160	1.11E-8	5.03	1.12E-8	5.02	1.24E-8	5.02	1.09E-8	5.02
200	3.64E-9	5.01	3.67E-9	4.99	4.07E-9	4.99	3.56E-9	5.04

Table 2: Order of accuracy for (4.2) with  $u(x,y,t=0) = \sin(x+y)$  at  $T=20$ .  $CFL=2.2$ .

-	Method I		Method II		Method III		Method IV	
	error	order	error	order	error	order	error	order
20×20	7.94E-4	-	7.94E-4	-	8.28E-4	-	6.03E-4	-
40×40	2.51E-5	4.98	2.51E-5	4.98	2.62E-5	4.97	2.24E-5	4.75
60×60	3.29E-6	5.01	3.29E-6	5.01	3.44E-6	5.00	3.10E-6	4.88
80×80	7.80E-7	5.00	7.80E-7	5.00	8.16E-7	5.00	7.50E-7	4.93

Four different SL FD methods (Methods I, II, III, IV) with fifth order WENO reconstruction/interpolation are used to solve Eq. (4.1). Table 1 gives the  $L^1$  error, and the corresponding order of convergence when the four different methods are applied to Eq. (4.1) with the smooth initial data  $u(x,0) = \sin(x)$ . As expected, fifth order convergence is observed. The schemes also inherit the essentially non-oscillatory property of the WENO reconstruction, when advecting rectangular waves. Numerical results are omitted here to save space. For Method IV, the conservation error is not significant for this example. The conservation error up to  $T=20$  is in the order of  $10^{-15}$  for the smooth sine wave function, and is in the order of  $10^{-12}$  for the rectangular wave. The non-conservative scheme seems to have slightly smaller  $L^1$  error in magnitude.

**Example 4.2.** (Two dimensional linear transport)

$$u_t + u_x + u_y = 0, \quad x \in [0, 2\pi], \quad y \in [0, 2\pi]. \quad (4.2)$$

The equation is being split into two one-dimensional equations, each of which is evolved by SL FD WENO methods. For any 2-D linear transport equation, the SL method is essentially a shifting procedure. Since the  $x$ -shifting and  $y$ -shifting operators commute, there is no dimensional splitting error in time and the spatial error is the dominant error. Table 2 gives the  $L^1$  error and the corresponding order of convergence for applying the four different SL FD schemes to Eq. (4.2) with the smooth solution  $u(x,y,t) = \sin(x+y-2t)$ . Again fifth order convergence for all schemes are observed as expected. In our 2-D simulation,  $CFL = \Delta t / \Delta x + \Delta t / \Delta y$ .

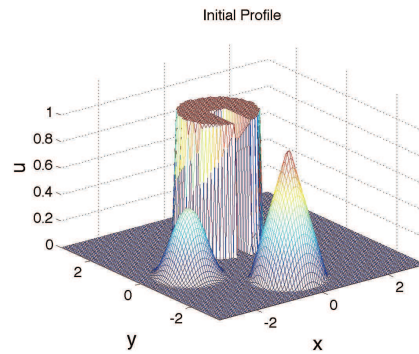


Figure 1: Plots of the initial profile. The numerical mesh is  $100 \times 100$ .

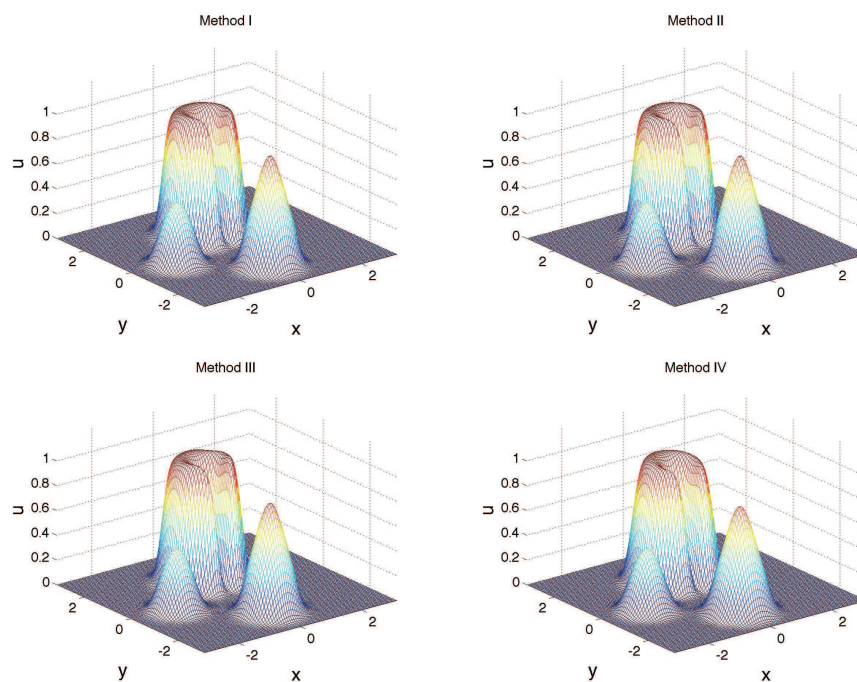


Figure 2: Plots of the numerical solution for Eq. (4.3) with  $CFL=2.2$  at  $T=12\pi$ . The numerical mesh is  $100 \times 100$ . From left to right, from top to bottom are the solutions from Methods I, II, III, IV respectively.

**Example 4.3.** (Rigid body rotation)

$$u_t - yu_x + xu_y = 0, \quad x \in [-2\pi, 2\pi], \quad y \in [-2\pi, 2\pi]. \tag{4.3}$$

The equation is being Strang split into two one-dimensional equations, each of which is evolved by different SL FD WENO methods. The initial condition we used is plotted in Fig. 1. It includes a slotted disk, a cone as well as a smooth hump, similar to the one in [18] for comparison purpose. The numerical solutions after six full revolutions by the schemes are plotted in Fig. 2 by 2D surfaces and in Fig. 3 by 1D cuts benchmarked with

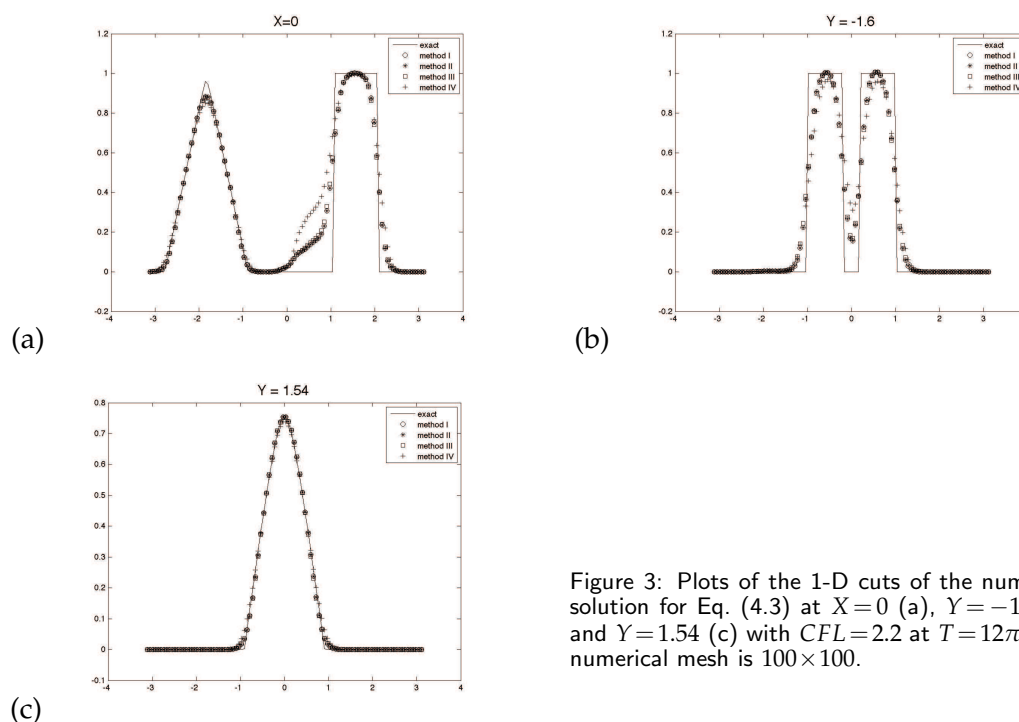


Figure 3: Plots of the 1-D cuts of the numerical solution for Eq. (4.3) at  $X=0$  (a),  $Y=-1.6$  (b) and  $Y=1.54$  (c) with  $CFL=2.2$  at  $T=12\pi$ . The numerical mesh is  $100 \times 100$ .

the exact solution. With all the reconstructions, non-oscillatory capturing of discontinuities is observed. Conservative schemes (Methods I, II, III) are observed to perform better than the non-conservative SL FD WENO scheme (Method IV), see the first and second plots in Fig. 3.

## 5 The Vlasov-Poisson system

In this section, we demonstrate the performance of the proposed method, compared with those in [3, 21, 22] by applying them to classical problems in plasma physics, such as Landau damping and two-stream instability. These classical phenomena are described by the well-known Vlasov-Poisson (VP) system,

$$\frac{\partial f}{\partial t} + \mathbf{v} \cdot \nabla_{\mathbf{x}} f + \mathbf{E}(t, \mathbf{x}) \cdot \nabla_{\mathbf{v}} f = 0, \quad (5.1a)$$

$$\mathbf{E}(t, \mathbf{x}) = -\nabla_{\mathbf{x}} \phi(t, \mathbf{x}), \quad -\Delta_{\mathbf{x}} \phi(t, \mathbf{x}) = \rho(t, \mathbf{x}). \quad (5.1b)$$

In Eq. (5.1a)-(5.1b),  $\mathbf{x}$  and  $\mathbf{v}$  are coordinates in phase space  $(\mathbf{x}, \mathbf{v}) \in \mathbb{R}^3 \times \mathbb{R}^3$ ,  $\mathbf{E}$  is the electric field,  $\phi$  is the self-consistent electrostatic potential and  $f(t, \mathbf{x}, \mathbf{v})$  is the probability distribution function which describes the probability of finding a particle with velocity  $\mathbf{v}$  at position  $\mathbf{x}$  at time  $t$ . The probability distribution function couples to the long range fields

via the charge density,  $\rho(t, \mathbf{x}) = \int_{\mathbb{R}^3} f(t, \mathbf{x}, \mathbf{v}) d\mathbf{v} - 1$ , where we take the limit of uniformly distributed infinitely massive ions in the background. Eqs. (5.1a) and (5.1b) have been nondimensionalized so that all physical constants are one. Below, we briefly recall some classical preservation results in the VP system. We hope that our numerical solutions can preserve these classical conserved quantities as much as possible.

1. Preservation of the  $L^p$  norm, for  $1 \leq p < \infty$ ,

$$\frac{d}{dt} \int_v \int_x f(x, v, t)^p dx dv = 0. \tag{5.2}$$

2. Preservation of the entropy

$$\frac{d}{dt} \int_v \int_x f(x, v, t) \ln(f(x, v, t)) dx dv = 0. \tag{5.3}$$

3. Preservation of the energy

$$\frac{d}{dt} \left( \int_v \int_x f(x, v, t) v^2 dx dv + \int_x E^2(x, t) dx \right) = 0. \tag{5.4}$$

The Strang splitting SL method for the VP system was originally proposed in reference [4], and soon gained wide popularity [9, 10, 29]. The Strang splitting reduces the high dimensional nonlinear Vlasov equation into one-dimensional advection equations, on which the high order SL FD WENO schemes can be applied. In this section, the four different SL formulations tested in Section 4 are applied to the Strang splitted Vlasov equation. The schemes are tested in the classical problems in plasma physics, such as Landau damping, two stream instabilities. The performance of the schemes will be demonstrated/compared by the solution profiles, as well as by tracking the time evolution of theoretically preserved quantities (Eq. (5.2)-(5.4)) in the discrete sense.

Without loss of generality, we consider the Vlasov equation, Eq. (5.1a), with only one position and one velocity axis, i.e.,  $(x, v) \in \mathbb{R} \times \mathbb{R}$ . The extension to higher dimensions in  $\mathbf{x}$  and  $\mathbf{v}$  is straightforward. The time splitting form of Eq. (5.1a) is,

$$\frac{\partial f}{\partial t} + v \frac{\partial f}{\partial x} = 0, \tag{5.5a}$$

$$\frac{\partial f}{\partial t} + E(t, x) \frac{\partial f}{\partial v} = 0. \tag{5.5b}$$

The split form of Eq. (5.1a) can be made second order accurate in time by solving Eq. (5.5a) for a half time step, then solving Eq. (5.5b) for a full time step, followed by solving Eq. (5.5a) for a second half time step. The observation that both Eq. (5.5a) and Eq. (5.5b) are linear hyperbolic equations allows for a direct implementation of the SL FD WENO schemes. Specifically, the numerical update from  $f^n(x, v)$  (the solution at  $t^n = n\Delta t$ ) to  $f^{n+1}(x, v)$  is as follows:

1. Advance a half time step for Eq. (5.5a) by a SL method,

$$f^*(x, v) = \mathcal{SL}\left(f, \frac{1}{2}\Delta t\right); \quad (5.6)$$

2. Compute the electric field at the half step by substituting  $f^*$  into Eq. (5.1b) and solve for  $E^*(x)$ ;
3. Advance a full time step for Eq. (5.5b) by a SL method,

$$f^{**}(x, v) = \mathcal{SL}(f^*, \Delta t); \quad (5.7)$$

4. Advance a half time step for Eq. (5.5a) by a SL method,

$$f^{n+1}(x, v) = \mathcal{SL}\left(f^{**}, \frac{1}{2}\Delta t\right). \quad (5.8)$$

In our experiments, periodic boundary conditions are imposed in the  $x$ -direction and zero boundary conditions are imposed in the  $v$ -direction for all of our test problems. Because of the periodicity in space, a fast Fourier transform (FFT) is used to solve the 1-D Poisson equation.  $\rho(x, t)$  is computed by rectangular rule,

$$\rho(x, t) = \int f(x, v, t) dv = \sum_j f(x, v_j, t) \Delta v,$$

which is spectrally accurate [1], when the underlying function is smooth enough. In our numerical experiments below, The  $L^p$  norms/entropy/energy are numerically approximated by rectangular rule, which is again spectrally accurate, if the integrated function is smooth enough.

**Example 5.1.** (Weak Landau damping) Consider the example of weak Landau damping for the VP system. The initial condition used here is,

$$f(x, v, t=0) = \frac{1}{\sqrt{2\pi}} [1 + \alpha \cos(kx)] \exp\left(-\frac{v^2}{2}\right), \quad (5.9)$$

with  $\alpha = 0.01$  and  $k = 0.5$ . The time evolution of the  $L^2$  and  $L^\infty$  norm of the electric field is plotted in the upper plots of Fig. 4. The correct damping of the electric field is observed in the plots, benchmarked with the theoretical value  $\gamma = 0.1533$  [11] (the solid line in the same plots). We observe that all of the four methods generate very consistent results, performing very well in recovering the damping rate. We remark that the numerical results from the Method I, II and III are comparable with each other, almost indistinguishable from the plots in this example and other examples below in most cases. The time evolution of the  $L^1$ ,  $L^2$  solution norms, energy, entropy in the discrete sense are demonstrated in the mid and bottom plots in Fig. 4. The advantage of using conservative scheme in preserving the relevant physical norms is observed. Despite this, we remark that in the weak Landau damping case, the relevant physical norms are preserved pretty well for both the conservative and non-conservative schemes (see the magnitude variance in all of the  $y$ -axis) in Fig. 4.

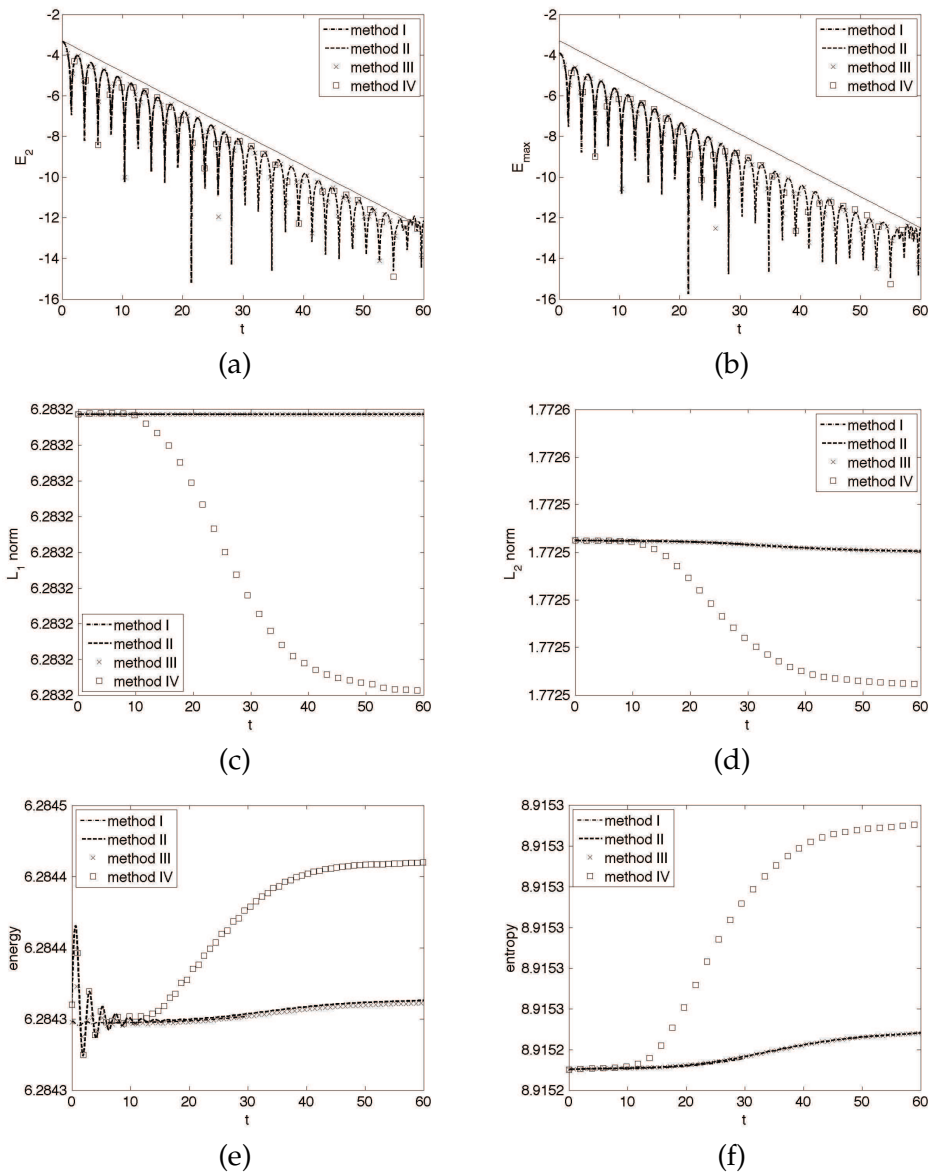


Figure 4: Weak Landau damping: time evolution of electric field in  $L^2$  (a) and  $L^\infty$  (b) norm,  $L^1$  (c) and  $L^2$  (d) norms of the solution as well as the discrete kinetic energy (e) and entropy (f).

**Example 5.2. (Strong Landau damping)** The next example we consider is the case of strong Landau damping. We simulate the VP system with the initial condition in Eq. (5.9) with  $\alpha=0.5$  and  $k=0.5$ . Our numerical simulation parameters for all schemes are  $v_{\max}=5$ ,  $N_x=64$ ,  $N_v=128$  and  $\Delta t=\Delta x$ ; where  $v_{\max}$  is the maximum velocity on the phase space mesh,  $N_x$  is the number of grid points along the  $x$  axis,  $N_v$  is the number of grid points along the  $v$  axis, and  $\Delta t$  is the time step used. In the first row of Fig. 5, the time evolu-

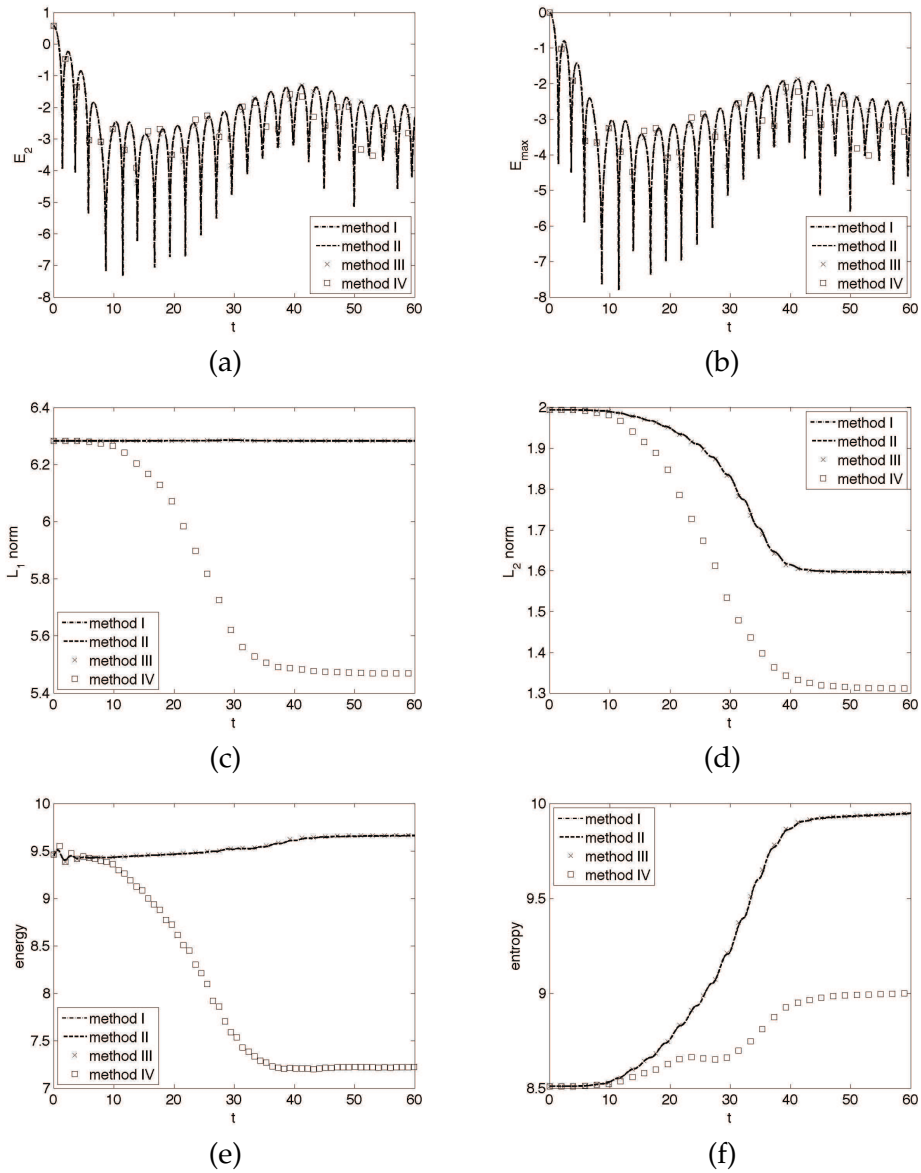


Figure 5: Strong Landau damping: time evolution of electric field in  $L^2$  (a) and  $L^\infty$  (b) norm,  $L^1$  (c) and  $L^2$  (d) norms of the solution as well as the discrete kinetic energy (e) and entropy (f).

tion of the  $L^2$  and  $L^\infty$  norm of the electric field is plotted. The profile of non-conservative Method IV deviates from the evolution profiles of other conservative SL FD WENO methods after longer time evolution (roughly around  $T = 40$ ). The discrete  $L^1$  norm,  $L^2$  norm, kinetic energy and entropy for four different methods are plotted in the second and third row of Fig. 5. It is observed that schemes with conservative properties do a better job in

preserving the discrete  $L^1, L^2$  norm and kinetic energy than a non-conservative scheme. On the other hand, the non-conservative scheme (Method IV) seems to be better in preserving the entropy, an observation that the authors could not explain. Since the numerical solutions we obtained are consistent with the Fig. 4.9 in [21], we skip demonstrating them to save space.

**Example 5.3.** (Two stream instability [11]) Consider the symmetric warm two stream instability, i.e., the electron distribution function in the VP system is started with the unstable initial condition [11],

$$f(x, v, t=0) = \frac{2}{7\sqrt{2\pi}}(1+5v^2) \left(1 + \frac{\alpha}{1.2}((\cos(2kx) + \cos(3kx)) + \cos(kx))\right) \exp\left(-\frac{v^2}{2}\right), \quad (5.10)$$

with  $\alpha = 0.01, k = 0.5$ . The length of the domain in the  $x$  direction is  $L = 2\pi/k$  and the background ion distribution function is fixed, uniform and chosen so that the total net charge density for the system is zero. Our numerical simulation parameters are  $v_{\max} = 5, N_x = 64, N_v = 128, \Delta t = \Delta x$  for all schemes. Fig. 6 shows numerical solutions of phase space profiles at  $T = 53$  from the four different SL FD WENO schemes. The conservative scheme (Method I, II, III) seem to perform slightly better than a non-conservative scheme, if careful observation in the rotational core is made. In the first row of Fig. 7, the time evolution

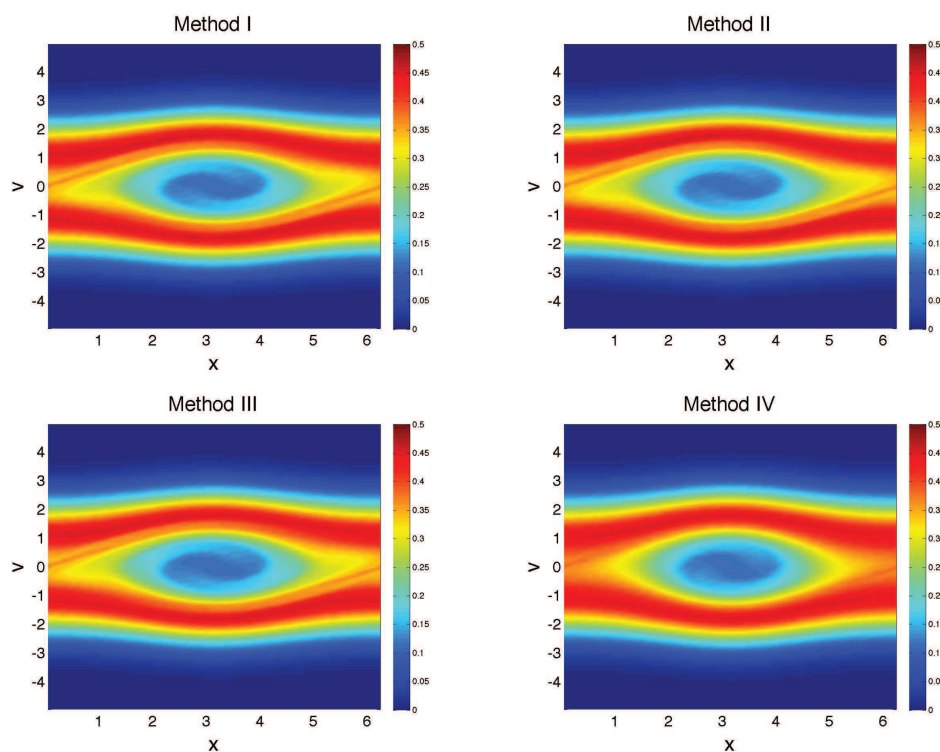


Figure 6: Phase space plots of the two stream instability at  $T = 53$  using Method I, II, III, IV. The numerical mesh is  $64 \times 128$ .

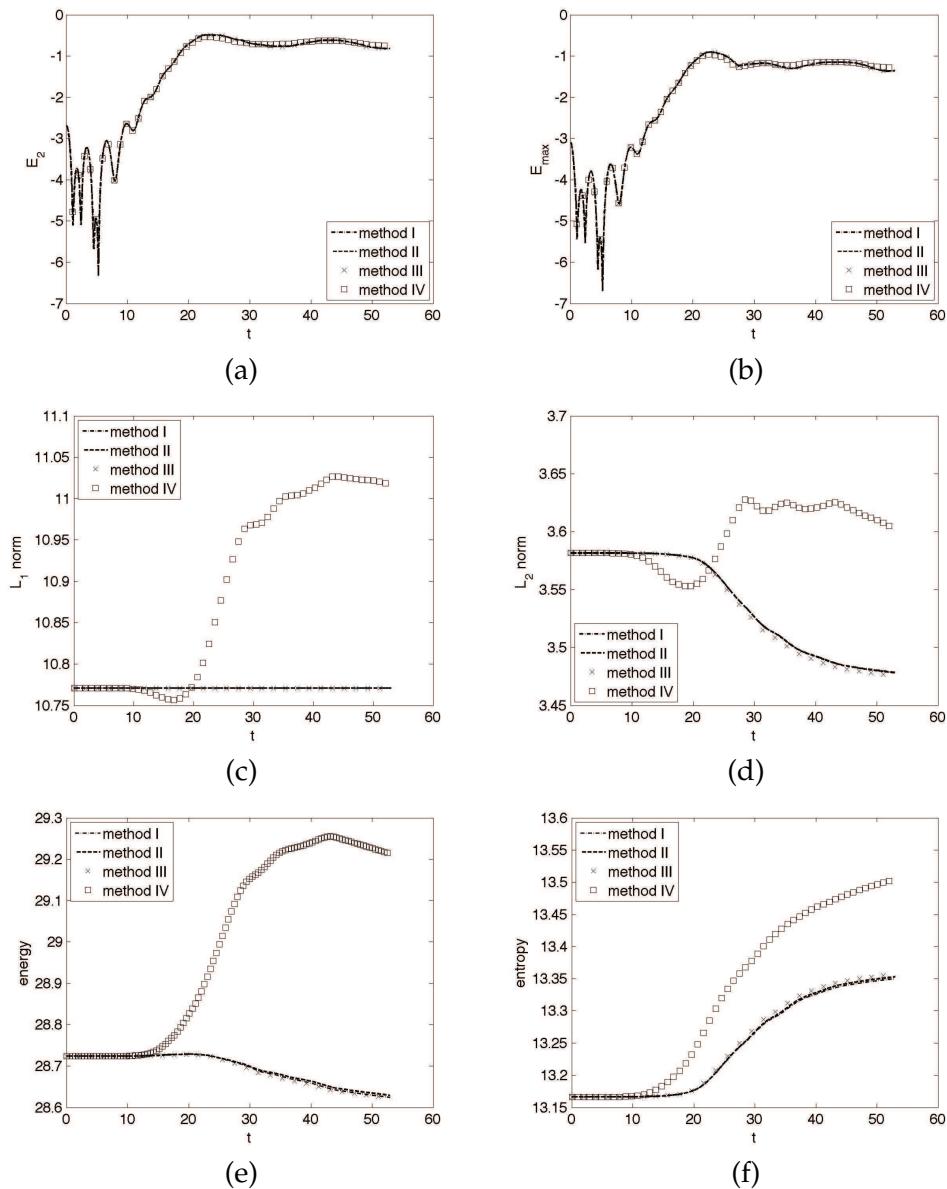


Figure 7: Two-stream instability: time evolution of electric field in  $L^2$  (a) and  $L^\infty$  (b) norm,  $L^1$  (c) and  $L^2$  (d) norms of the solution as well as the discrete kinetic energy (e) and entropy (f).

of the  $L^2$  and  $L^\infty$  norm of the electric field is plotted. Consistent numerical solutions from all of the four methods are observed. The second and third rows of Fig. 7 are the time development of the discrete  $L^1$  norm,  $L^2$  norm, kinetic energy and entropy for four different methods. It is observed that schemes with conservative properties in general do a better job in preserving those physical norms than a non-conservative scheme.

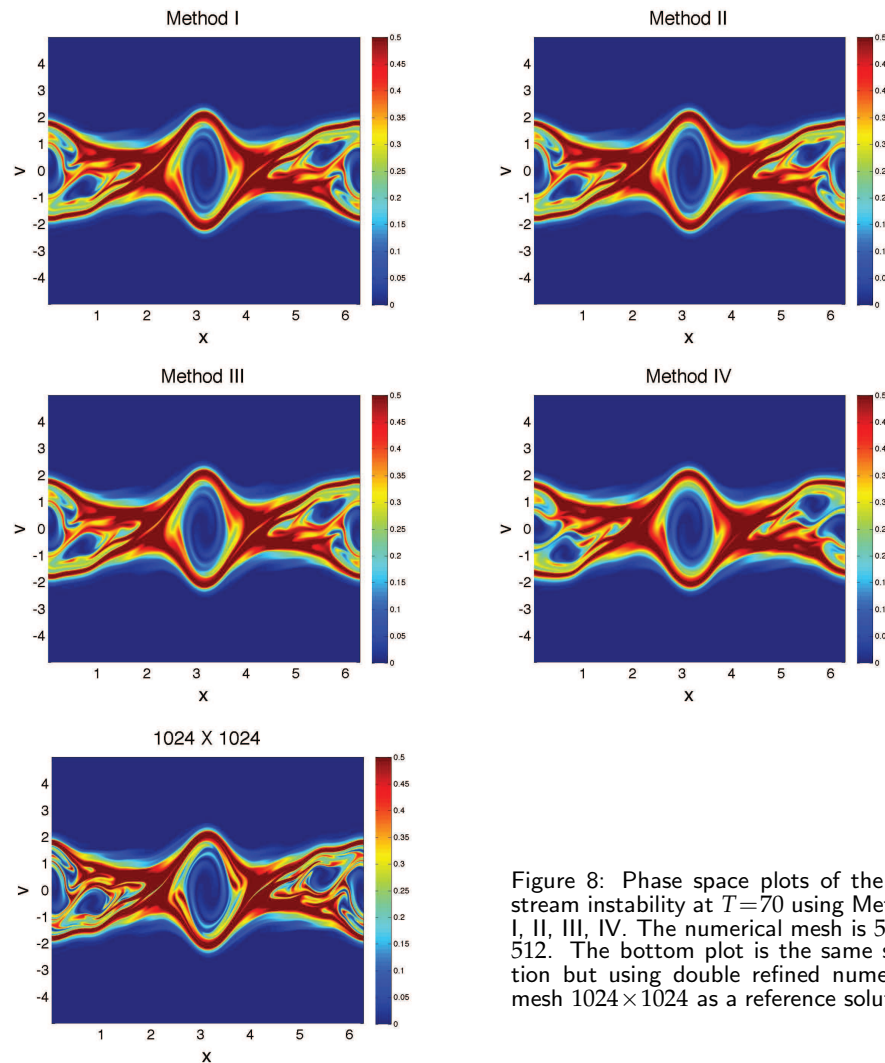


Figure 8: Phase space plots of the two stream instability at  $T=70$  using Method I, II, III, IV. The numerical mesh is  $512 \times 512$ . The bottom plot is the same solution but using double refined numerical mesh  $1024 \times 1024$  as a reference solution.

**Example 5.4.** (Two stream instability [9]) Consider the symmetric two stream instability, similar as in [9],

$$f(x, v, t=0) = \frac{1}{2v_{th}\sqrt{2\pi}} \left[ \exp\left(-\frac{(v-u)^2}{2v_{th}^2}\right) + \exp\left(-\frac{v+u}{2v_{th}^2}\right) \right] (1 + 0.05\cos(kx)), \quad (5.11)$$

with  $u = 0.99$ ,  $v_{th} = 0.3$  and  $k = 2/13$ . The background ion distribution function is fixed, uniform and chosen so that the total net charge density for the system is zero. Our numerical simulation parameters are  $v_{max} = 5$ ,  $N_x = 512$ ,  $N_v = 512$ ,  $\Delta t = \Delta x$  for all schemes. Fig. 8 shows numerical solutions of phase space profiles at  $T=70$  from the four different SL FD WENO schemes. The conservative scheme (Method I, II, III) seem to perform better than a non-conservative scheme, compared with the double refined reference solution, the last

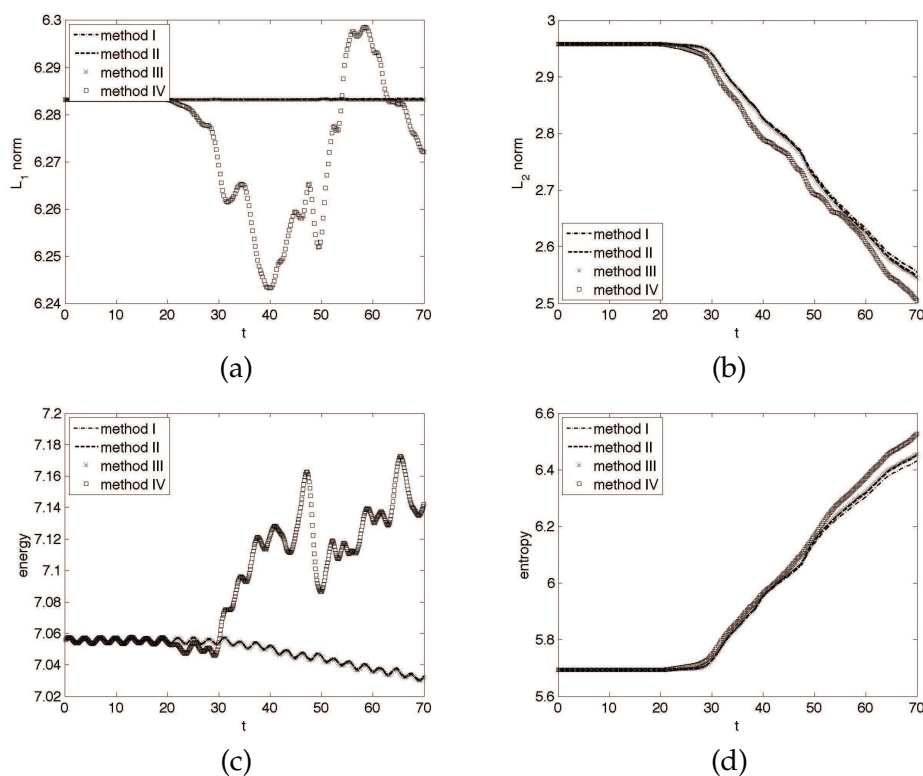


Figure 9: Two-stream instability: time evolution of  $L^1$  (a) and  $L^2$  (b) norms of the solution as well as the discrete kinetic energy (c) and entropy (d).

plot in Fig. 8. In the first row of Fig. 9, the time evolution of the  $L^2$  and  $L^\infty$  norm of the electric field is plotted. Consistent numerical solutions from all of the four methods are observed. The second and third rows of Fig. 9 are the time development of the discrete  $L^1$  norm,  $L^2$  norm, kinetic energy and entropy for four different methods. Again, conservative schemes in general perform better in preserving those physical norms than a non-conservative scheme.

## 6 Conclusions

In this paper, we propose a new conservation semi-Lagrangian (SL) finite difference (FD) WENO scheme, based on the same reconstruction procedure as the one used in a SL finite volume (FV) WENO scheme. We implement the proposed scheme, as well as the other three SL FD WENO schemes in [3,21,22] to the linear advection, rigid body rotation problem; and on the Landau damping and two-stream instabilities by solving the VP system. We compare the performance of different schemes, and demonstrate that conservative schemes in general perform better than non-conservative ones in tracking the evolution of physically conserved quantities.

## Acknowledgments

The research of J.-M. Qiu is supported by AFOSR grant FA9550-09-1-0344 and NSF grant DMS-0914852. The research of C.-W. Shu is supported by AFOSR grant FA9550-09-1-0126 and NSF grant DMS-0809086.

## References

- [1] J. P. Boyd, *Chebyshev and Fourier Spectral Methods*, Courier Dover Publications, 2001.
- [2] E. Carlini, R. Ferretti, and G. Russo, A weighted essentially nonoscillatory, large time-step scheme for Hamilton-Jacobi equations, *SIAM J. Sci. Comput.*, 27(3) (2006), 1071–1091.
- [3] J. A. Carrillo and F. Vecil, Nonoscillatory interpolation methods applied to Vlasov-Based models, *SIAM J. Sci. Comput.*, 29 (2007), 1179–1206.
- [4] C. Z. Cheng and G. Knorr, The integration of the Vlasov equation in configuration space, *J. Comput. Phys.*, 22(3) (1976), 330–351.
- [5] P. N. Childs and K. W. Morton, Characteristic Galerkin methods for scalar conservation laws in one dimension, *SIAM J. Numer. Anal.*, 27(3) (1990), 553–594.
- [6] B. Cockburn, C. Johnson, C.-W. Shu, and E. Tadmor, *Advanced Numerical Approximation of Nonlinear Hyperbolic Equations*, Springer, New York, 1998.
- [7] P. Colella and P. R. Woodward, The piecewise parabolic method (PPM) for gas-dynamical simulations, *J. Comput. Phys.*, 54(1) (1984), 174–201.
- [8] N. Crouseilles, G. Lattu, and E. Sonnendrücker, Hermite spline interpolation on patches for parallelly solving the Vlasov-Poisson equation, *Int. J. Appl. Math. Comput. Sci.*, 17(3) (2007), 335–349.
- [9] N. Crouseilles, M. Mehrenberger, and E. Sonnendrücker, Conservative semi-Lagrangian schemes for Vlasov equations, *J. Comput. Phys.*, 229(6) (2010), 1927–1953.
- [10] F. Filbet and E. Sonnendrücker, Comparison of eulerian Vlasov solvers, *Comput. Phys. Commun.*, 150(3) (2003), 247–266.
- [11] F. Filbet and E. Sonnendrücker, Comparison of Eulerian Vlasov solvers, *Comput. Phys. Commun.*, 150(3) (2003), 247–266.
- [12] F. Filbet, E. Sonnendrücker, and P. Bertrand, Conservative numerical schemes for the Vlasov equation, *J. Comput. Phys.*, 172(1) (2001), 166–187.
- [13] F. Filbet, E. Sonnendrücker, and P. Bertrand, Conservative numerical schemes for the Vlasov equation. *J. Comput. Phys.*, 172(1) (2001), 166–187.
- [14] S. Gottlieb, D. I. Ketcheson, and C.-W. Shu, High order strong stability preserving time discretizations, *J. Sci. Comput.*, 38(3) (2009), 251–289.
- [15] F. Huot, A. Ghizzo, P. Bertrand, E. Sonnendrücker, and O. Coulaud, Instability of the time splitting scheme for the one-dimensional and relativistic Vlasov-Maxwell system, *J. Comput. Phys.*, 185(2) (2003), 512–531.
- [16] G.-S. Jiang and C.-W. Shu, Efficient implementation of weighted ENO schemes, *J. Comput. Phys.*, 126(1) (1996), 202–228.
- [17] T. Lee and C. L. Lin, A characteristic Galerkin method for discrete Boltzmann equation, *J. Comput. Phys.*, 171(1) (2001), 336–356.
- [18] R. J. LeVeque, High-resolution conservative algorithms for advection in incompressible flow, *SIAM J. Numer. Anal.*, (1996), 627–665.

- [19] S. J. Lin and R. B. Rood, An explicit flux-form semi-Lagrangian shallow-water model on the sphere, *Quart. J. Royal. Meteorologic. Soc.*, 123(544) (1997), 2477–2498.
- [20] Y. Liu, C.-W. Shu, and Zhang M, On the positivity of linear weights in WENO approximations, *Acta. Math. Appl. Sin.*, 25 (2009), 503–538.
- [21] J.-M. Qiu and A. Christlieb, A Conservative high order semi-Lagrangian WENO method for the Vlasov Equation, *J. Comput. Phys.*, 229(4) (2010), 1130–1149.
- [22] J.-M. Qiu and C.-W. Shu, Conservative high order semi-Lagrangian finite difference WENO methods for advection in incompressible flow, *J. Comput. Phys.*, 230 (2011), 863–889.
- [23] J.-M. Qiu and C.-W. Shu, Convergence of Godunov-type schemes for scalar conservation laws under large time steps, *SIAM J. Numer. Anal.*, 46 (2008), 2211–2237.
- [24] J.-X. Qiu and C.-W. Shu, Finite difference WENO schemes with Lax-Wendroff-type time discretizations, *SIAM J. Sci. Comput.*, 24(6) (2003), 2185–2200.
- [25] K. Sebastian and C.-W. Shu, Multidomain WENO finite difference method with interpolation at subdomain interfaces, *J. Sci. Comput.*, 19(1) (2003), 405–438.
- [26] C.-W. Shu, High order weighted essentially non-oscillatory schemes for convection dominated problems, *SIAM Rev.*, 51 (2009), 82–126.
- [27] E. Sonnendruecker, J. Roche, P. Bertrand, and A. Ghizzo, The semi-Lagrangian method for the numerical resolution of the Vlasov equation, *J. Comput. Phys.*, 149(2) (1999), 201–220.
- [28] H. Takewaki, A. Nishiguchi, and T. Yabe, Cubic interpolated pseudo-particle method (CIP) for solving hyperbolic-type equations, *J. Comput. Phys.*, 61(2) (1985), 261–268.
- [29] T. Umeda, M. Ashour-Abdalla, and D. Schriver, Comparison of numerical interpolation schemes for one-dimensional electrostatic Vlasov code, *J. Plasma. Phys.*, 72(06) (2006), 1057–1060.
- [30] D. Xiu and G. E. Karniadakis, A semi-Lagrangian high-order method for Navier-Stokes equations, *J. Comput. Phys.*, 172(2) (2001), 658–684.
- [31] T. Yabe, F. Xiao, and T. Utsumi, The constrained interpolation profile method for multiphase analysis, *J. Comput. Phys.*, 169(2) (2001), 556–593.